Deposition of nickel oxide by direct current reactive sputtering Effect of oxygen partial pressure

Arkadiusz Karpinski, Axel Ferrec, Mireille Richard-Plouet, Linda Cattin, Mohammed Abdou Djouadi, Luc Brohan, Pierre-Yves Jouan

Deposition of nickel oxide by direct current reactive sputtering Effect of oxygen partial pressure

A. Karpinski, A. Ferrec, M. Richard-Plouet, L. Cattin, M.A. Djouadi, L. Brohan, P.-Y. Jouan *

Institut des Matériaux Jean Rouxel, Université de Nantes, CNRS 2 rue de la Houssinière, BP 32229 44322 Nantes cedex 3, France

Nickel oxide thin films were deposited by Direct Current magnetron reactive sputtering from Ni target onto SnO_2:F conductive glass substrates. The process was carried out without intentional heating, in an argon/oxygen gas mixture with various oxygen contents and discharge currents. The polycrystalline NiO thin films were depos-ited with controlled growth of the structure along [111] and [200] crystallographic directions for chosen conditions. Morphology of as-deposited films was found to depend on the preferentially oriented NiO crystals. Moreover, on the basis of discharge voltage as a function of the O_2 partial pressure for a constant discharge current, we present here the method to estimate the deposition conditions allowing us to achieve the desired preferential growth of transparent p-type semiconductor NiO, by Direct Current magnetron reactive sputtering.

1. Introduction

NiO is a wide band gap p-type semiconductor and as a thin film it provides high transparency. Therefore, the deposition of such a material on transparent conductive glass substrate becomes interesting for development of electrochromic and photovoltaic devices where high transparency is needed.

In recent years, numerous methods have been used in order to deposit nickel oxide film such as metal organic chemical vapor deposition [1], thermal evaporation [2], sol–gel deposition [3], pulsed-laser-deposition [4] and intermittent spray pyrolysis process [5]. Among them, reactive magnetron sputtering is the most widely used [6–10]. The film properties and structure growth are affected by various deposition process parameters such as O_2 partial pressure in the gas mixture, total pressure, sputtering power, substrate temperature, etc. The predominant parameters are probably the partial pressure of O_2 in the gas mixture [11] and substrate temperature [12]. In this paper, the impact of O_2 partial pressure on plasma characteristics has been investigated. Indeed, we show in this paper that the preferred crystalline orientation is directly related to the amount of oxygen and monitoring this amount should enable us to control the film properties: transparency, conductivity (p or n)…

2. Experimental methods

The NiO thin films were deposited on SnO_2:F conducting glass ASAHI 120 by Direct Current reactive magnetron sputtering using a pure nickel target (99.99%) and an Ar–O_2 gas mixture. A 1.3 in. diameter (30 mm) target was used and substrates were placed at approximately 30 mm from this target. Thanks to mass flow controller, argon and oxygen gases could be adjusted. The resulting oxygen ratio in the fed gas was defined as: $O_2\% = V(O_2)/(V(O_2) + V(Ar))$ (where V represents the mass flow of each gas) and varied from 0 to 25%. The base pressure was about $2.7.10^{-4}$ Pa. In order to maintain the pumping speed constant, the turbo molecular pump valve was fully open. Then the discharge pressure in pure argon was 0.44 Pa and was modified from 0.45 to 0.51 Pa, depending on the oxygen content. Different discharge currents (110, 80 and 50 mA) were tested. Pre-sputtering process was done in two steps: first with argon to clean the target and second with the chosen working gases mixture in order to reach a steady state before deposition. The crystal structure of films, as a function of the thickness, was identified by X-Ray Diffraction (XRD) using a SIEMENS D 5000 diffractometer, in a grazing mode, for films close to 100 nm, (with a grazing angle 1° (θ), CuK_α radiation). Thicker films were analyzed using a Brüker D8 Advance powder diffractometer operating in Bragg–Brentano geometry (Ge monochromator, $CuK_{\alpha 1}$ $\lambda = 1.540598$ Å). The film morphology was examined by Scanning Electron Microscopy (SEM), using SEM Jeol JSM 7600F and JSM 6400F. The stoichiometry of thin films was evaluated by Energy-Dispersive Xray spectroscopy (EDX) equipment in a SEM Jeol 5800, operating at 7 kV. The film thickness was measured using a surface profilometer (DEKTAK 8). The electrical conductivity was measured, with the four-point probe technique, using copper electrode. The Hall effect measurements were

* Corresponding author.
E-mail address: pierre-yves.jouan@cnrs-imn.fr (P.-Y. Jouan).

performed utilizing the Van der Paw arrangement. The majority carrier type has been checked using the hot probe technique.

3. Results and discussion

3.1. Estimation of the deposition conditions

There are three basic feedback signals for controlling the reactive process during sputter deposition: mass spectrometry [13], optical emission spectroscopy [14] and cathode voltage (i.e. discharge voltage) [15]. In this study, we analyzed the electrical signal of the cathode because it is an easy handling technique giving fast updated information (potentially less than a few milliseconds). The signal strongly depends on the properties of the material which is formed on the cathode surface during the sputtering process [16]. The behavior of the cathode voltage was studied by increasing the oxygen content (Fig. 1a) with fixed values of current and flow of inert gas (10 sccm, standard cubic centimeter per minute, of Argon). In Fig. 1a, we can also observe that increasing the discharge current leads to a shift of the curve toward higher oxygen flux. Indeed, the discharge current is the sum of both electron and ion current (Ar^+ created by electron collisions near the cathode). Intensifying the ion current leads to an increase of the sputtering of the target, thus, as expected or as generally reported, the oxygen partial pressure required to observe the oxidation of the cathode is higher. In general, the influence of the reactive gas content on the discharge voltage, leads to 2 regions, related to the target state: metallic or poisoned [17,18]. In the case of the nickel target, we differentiated 4 regimes, on the characteristic of discharge voltage (Fig. 1b). Each region exhibits a typical X-ray diffraction pattern in which the peaks intensities are significantly varying. A similar behavior of discharge voltage has been already observed by Hotovy et al. [6], but it was not clearly correlated to the preferential growth of NiO films. The 4 regimes are as follows:

- In the first region, the target is in a metallic state, the oxygen species reaching the target are removed by the ion bombardment, allowing the target to remain metallic and therefore the discharge voltage does not change significantly.
- In the second region, the target is in an intermediate state, the amount of oxygen reaching the target starts to become higher than the oxygen removed by sputtering. We observe an enhancement (absolute value) of the target potential which indicates a decrease in electrical conductivity of the cathode with a low increase of secondary electron emission coefficient.
- In the third region, the target potential seems to stabilize, suggesting that the cathode is in a semi-conductive state, due to the formation of NiO layer on the target surface. However this behavior is difficult to understand, some authors attribute this stabilization at high potential, for a critical oxygen partial pressure, to the formation of negative oxygen ions [19,20]. In fact near the cathode we have two electron populations [21], high energy electrons which can collide to O_2 molecules leading to dissociation–ionization (maximum of the cross section at about 100 eV [22]) of the O_2 molecules with the creation of low energy electrons increasing the second population of electrons which are thermalyzed (4 eV) and which can get attached to O atoms or O_2 molecules but also collide to O_2 molecules to form $2O^-$ (maximum of the cross section at about 6 eV [22]). These negative ions consume electrons and are not trapped by the magnetic field, hence we observe a diminution of the ionic density ($n_i = n_e$) in the plasma and thus, in order to maintain the discharge current, the cathode voltage increases.
- In the fourth region, the target is fully oxidized, the discharge voltage stabilized again at a lower (absolute value) discharge voltage. This is the so-called poisoned mode of the cathode. This low discharge voltage could be due to an increase in the secondary electron emission coefficient and in discharge pressure (oxygen is added).

During our experiments, the hysteresis loop (consumption by the walls) that normally occurs, when decreasing the reactive gas partial pressure, was not observed. This is probably due to the small surface of the cathode (1.3 in. in diameter) and the relatively high pumping speed (260 $L.s^{-1}$).

3.1.1. Deposition rate

The deposition rate is directly proportional to the sputtering yield which depends on the discharge current (i.e.: power) and on the oxidation degree of the cathode. Thus, the deposition rate appears to be a consequence of the discharge conditions, it could not be considered as

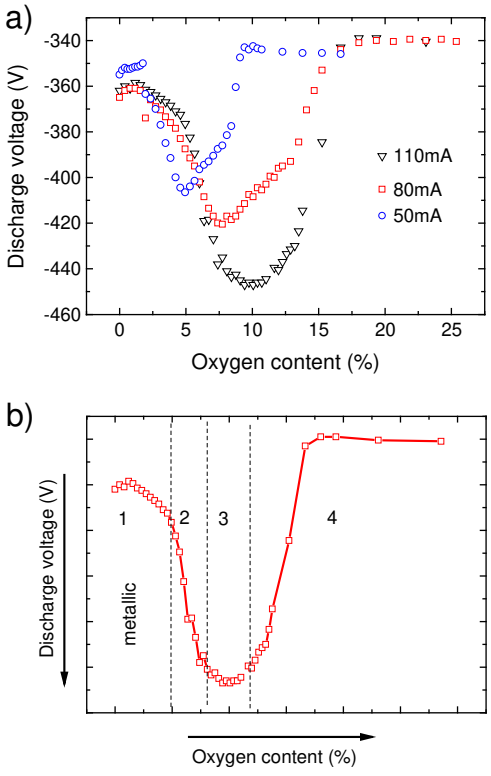

Fig. 1. Discharge voltage vs oxygen content for different discharge currents: a) experimental data, 50 mA blue circle, 80 mA red square, 110 mA black triangle, b) differentiation of 4 zones in the discharge curve (see text).

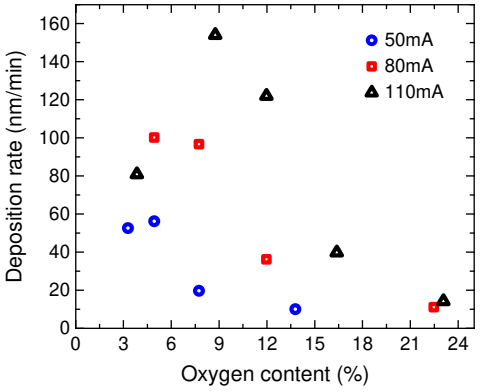

Fig. 2. Deposition rate for various evaluated discharge currents, 50 mA blue circle, 80 mA red square, 110 mA black triangle.

a parameter in this study. The experimental deposition rates of NiO as a function of oxygen content in the gas mixture for 3 discharge currents are presented in Fig. 2. The deposition rate augments with increasing discharge current as commonly observed. For each examined current, the deposition rate reaches a maximum in the semi-conductive region (zone 2) and then decreases strongly due to the low sputter yield of the oxide for zones 3 and 4. The same evolution of the deposition rate as a function of oxygen content has been observed by Liu et al. [23].

3.2. Crystallographic orientations

The structure of as-deposited NiO was found to be polycrystalline but with preferential orientations, strictly related to the oxygen content in the mixture of working gases (Fig. 3). The preferential growth of NiO was always correlated to the shape of the discharge current (Fig. 1b), and therefore to the oxygen partial pressure. The region defined as 1 was out of consideration because the deposited films were also composed of metallic nickel. The region 2 with relatively low oxygen content was accompanied by an increase in the (111) diffraction peak; region 3, where discharge voltage reached absolute maximum was related to structure growth of NiO with peak intensities close to standard JCPDS card (Bunsenite, NaCl-type structure, 2003 No: 89-7130) NiO powder-like structure; region 4, rich oxygen content was characterized by the predominance of the (200) peak intensity.

Films deposited in the oxygen range allowing transition of preferential growth from [111] to [200] directions exhibit intense and narrow diffraction peaks, however XRD diagrams of the deposits carried out in relatively high oxygen content show less intensity signal for films having similar thickness. This may indicate the presence of amorphous phase or a loss in the number of crystallite domains, due to a raise of

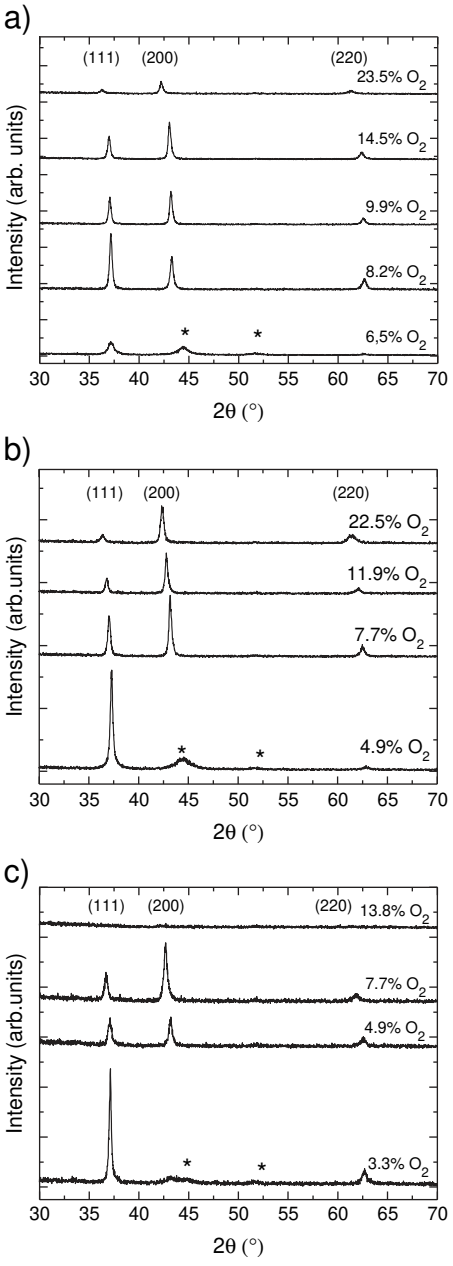

Fig. 3. XRD diagrams for 1 μm NiO thin films deposited at discharge currents: a) 110 mA, b) 80 mA and c) 50 mA. The peaks attributed to metallic nickel were marked by an asterisk (*).

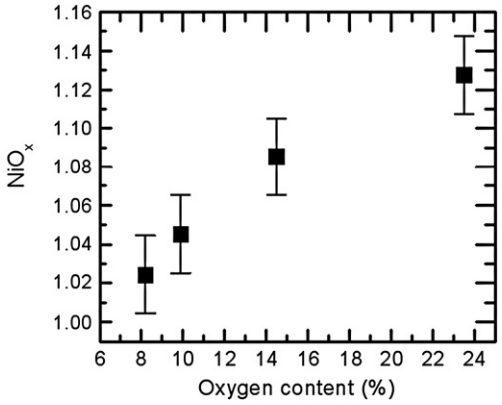

Fig. 4. Evolution of the stoichiometry for 1 μm NiO_x thin films deposited at 110 mA for various oxygen contents, calculated from EDX measurements.

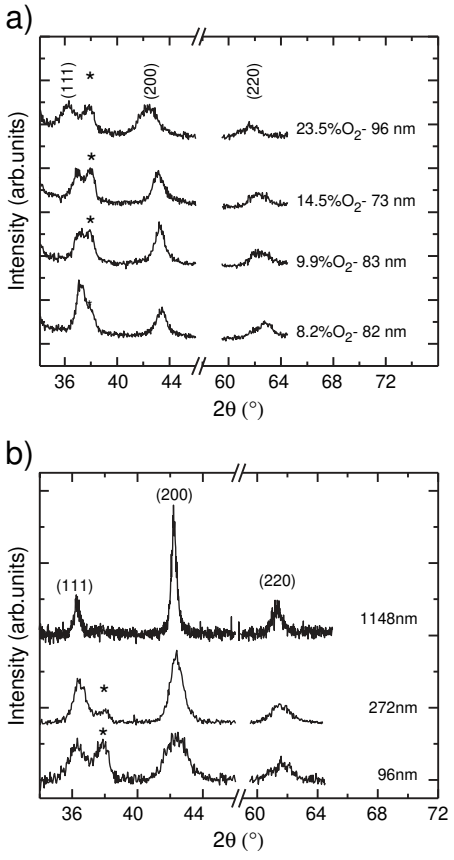

Fig. 5. XRD diagrams for NiO films deposited at the discharge current of 110 mA: a) of about 80 nm thicknesses for various oxygen content; b) deposited at 23.5% O_2 for different thicknesses. Peaks of SnO_2:F are marked by an asterisk (*).

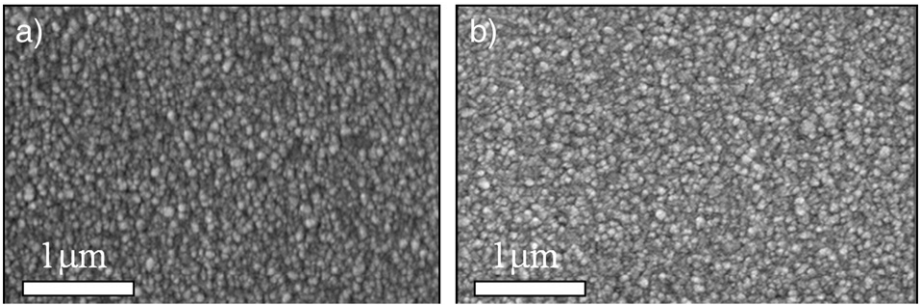

Fig. 6. Representative surface of 80 nm thin films deposited at 110 mA: a) 9.9% O_2, b) 23.5% O_2.

oxygen content in the mixture of working gases. Nevertheless, the non-stoichiometry in nickel, for example, may also produce the same effect, causing less X-rays diffraction from the heaviest Ni atoms. As plotted in Fig. 4, the O/Ni ratio of as deposited NiO films (supported by EDX analysis) suggests that some vacancies in nickel atoms occur leading to the formula: $NiO_{1.13}$, for high flux of oxygen gas. This non-stoichiometry is associated to a shift of the diffraction peaks toward low 2θ angles, indicating an expansion of the cell parameters. This observation is coherent with previously reported data concerning NiO obtained by spray pyrolysis from nickel nitrate [24].

Reported XRD results for NiO thin films deposited by reactive sputtering, show that increasing the temperature and/or the discharge power for a fixed oxygen flow rate leads to [111] preferential orientation. Note that in both cases (increasing the temperature and/or the discharge power) the effect on the film is a reduction of oxygen content which is consistent with our results [25–27].

Crystallographic studies of the deposits at lower thicknesses indicated that preferential growth of the NiO structure is not only affected by oxygen content but also depends on the thickness of thin films. Fig. 5a shows crystallographic reflections of samples at about 80 nm thickness, for increasing oxygen contents.

The intensity of the (111) peak decreases with increasing oxygen content from 8.2 to 9.9% O_2 (Fig. 4a). For the deposits at 14.5% or 23.5% O_2 the intensities of the (111) and (200) reflections are comparable. This gives an idea that at high oxygen content the grain growth process is competitive for all the directions, for very thin layers (lower than 100 nm) at high oxygen values. The structural evolution is clearly observed for samples deposited at 23.5% O_2 when the thickness of thin film enhances (Fig. 5b). At the thickness of 96 nm, both (111) and (002) grains are present. Further growth leads to progressive predominance of the growth along the [200] direction when the thickness reaches 272 nm and 1148 nm. Predominance of the preferential orientation with the thickness can be associated to competitive growth and grains coarsening. The thin film, at the very beginning of the growth, is randomly oriented while overall microstructure evolves toward a final well crystallized state (intense and narrow diffraction peaks) driven by the appropriate deposition conditions [9,10].

3.3. Morphology and cross-section

Fig. 6 shows a typical surface of 80 nm thin films deposited for various oxygen contents at 110 mA current. The surface appears composed of round grains with size ranging from 50 to 100 nm. When the NiO thickness grows to about 1 μm, grain coarsening is observed (Fig. 7).

Initial round grains evolve to flakes like crystals close to 300 nm for low oxygen contents (Fig. 7a). For high oxygen values (Fig. 7d), the surface aspect is different with rectangular and triangular grains in the size range close to 100 nm. We observe that this size evolution depends on the orientation: the grain narrowing is associated to film

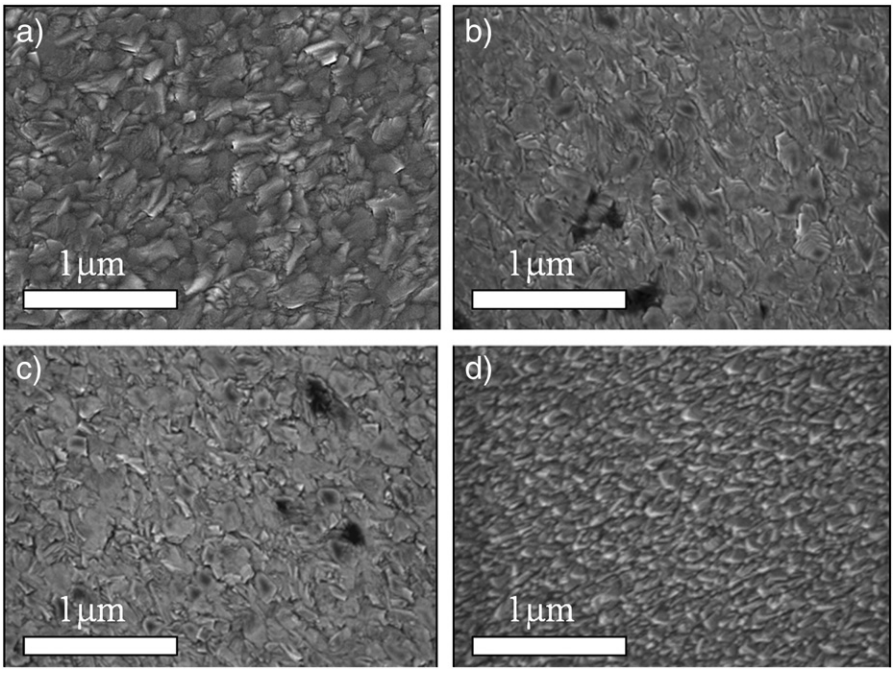

Fig. 7. Representative surface of 1 μm thin films deposited at 110 mA: a) 8.2% O_2, b) 9.9% O_2, c) 14.5% O_2, and d) at 23.5% O_2.

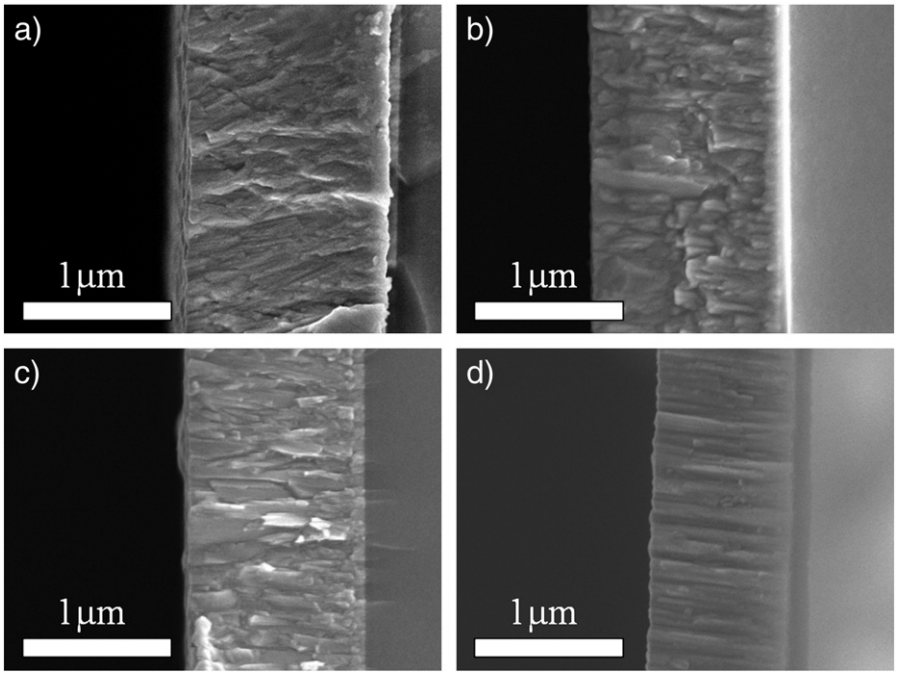

Fig. 8. Cross-section of 1 μm thin films deposited at 110 mA: a) 8.2% O_2, b) 9.9% O_2, c) 14.5% O_2, and d) at 23.5% O_2.

growth along the [200] direction. Cross-section images (Fig. 8) reveal the columnar nature of the films in every case. The sample deposited at lowest oxygen value grows as columns with limited extension and different growth directions, leading to low ordering of the microstructure. Deposited NiO at 9.9 and 14.5% O_2 is also composed of columns, expanding during nucleation process, which is affected by competitive growth along both preferential orientations. Such a type of growth is often accompanied by the formation of intercolumnar voids (see Fig. 7b, c). Sample deposited at high oxygen flow (Fig. 8d) consists in highly ordered cylindrical grains having mainly the [200] orientation.

4. Conclusions

Nickel oxide thin films were deposited onto conductive transparent glass substrates. The optimization of deposition conditions allowed us to control the preferential structure growth along [111] or [200] direction in a continuous manner as a function of the oxygen content in the mixture of working gases. Whatever the experimental conditions, the discharge voltage characteristic presents an unusual shape with a local maximum. The position of this maximum is shifted toward higher oxygen percentages when the current increases. The deposition conditions allowed us to tune the polycrystalline microstructure and preferentially oriented growth could be observed. Finally, we have checked that the NiO semi-conductor films are p-type and their resistivity ρ, is around 2 Ω.cm. The UV–Visible measurements have already been reported. The optical band gap lies between 3.2 and 4 eV, as expected, with a transparency up to 80% [28].

Acknowledgments

This work was financially supported by the French Research Agency (ANR) through the SOLHYPIN project. The authors would like to thank Dr. M. Morsli from the University of Nantes for electrical measurements and N. Stephant from the CMC-University of Nantes for SEM observations.

References

[1] K.-C. Min, M. Kim, Y.-H. You, S.S. Lee, Y.K. Lee, T.-M. Chung, C.G. Kim, J.-H. Hwang, K.-S. An, N.-S. Lee, Y. Kim, Surf. Coat. Technol. 201 (2007) 9252.
[2] I. Porqueras, E. Bertran, Thin Solid Films 398–399 (2001) 41.
[3] Yi-Mu Lee, Cheng-Hsing Hsu, Hung-Wei Chen, Appl. Surf. Sci. 255 (2009) 4658.
[4] B. Sasi, K.G. Gopchandran, Sol. Energy Mater. Sol. Cells 91 (2007) 1505.
[5] B.A. Reguig, A. Khelil, L. Cattin, M. Morsli, J.C. Bernede, Appl. Surf. Sci. 253 (2007) 4330.
[6] I. Hotovy, J. Huran, J. Janik, A.P. Kobzev, Vacuum 51 (1998) 157.
[7] H. Sato, T. Minami, S. Takata, T. Yamada, Thin Solid Films 236 (1993) 27.
[8] M. Kitao, K. Izawa, K. Urabe, T. Komatsu, S. Kuwano, S. Yamada, Jpn. J. Appl. Phys. 33 (1994) 6656.
[9] B. Subramanian, M. Mohamed Ibrahim, V. Senthilkumar, K.R. Murali, V.S. Vidhya, C. Sanjeeviraja, M. Jayachandran, Physica B 403 (2008) 4104.
[10] Jiin-Long Yang, Yi-Sheng Lai, J.S. Chen, Thin Solid Films 488 (2005) 242.
[11] I. Hotovy, J. Huran, L. Spiess, S. Hascik, V. Rehacek, Sens. Actuators, B 57 (1999) 147.
[12] H.-L. Chen, Y.-M. Lu, W.-S. Hwang, Surf. Coat. Technol. 198 (2005) 138.
[13] V. Vancoppenolle, P.-Y. Jouan, M. Wautelet, J.-P. Dauchot, M. Hecq, J. Vac. Sci. Technol., A 17 (1999) 3317.
[14] V. Vancoppenolle, P.-Y. Jouan, A. Ricard, M. Wautelet, J.-P. Dauchot, M. Hecq, Appl. Surf. Sci. 205 (2003) 249.
[15] W.D. Sproul, D.J. Christie, D.C. Carter, Thin Solid Films 491 (2005) 1.
[16] D. Depla, S. Mahieu, R. De Gryse, Thin Solid Films 517 (2009) 2825.
[17] G. Mohan Rao, S. Mohan, J. Appl. Phys. 69 (9) (1991) 6652.
[18] I. Safi, Surf. Coat. Technol. 127 (2000) 203.
[19] S. Maniv, W.D. Westwood, J. Vac. Sci. Technol. 17 (1980) 743.
[20] A. Rizk, S.B. Youssef, S.K. Habib, Vacuum 38 (1988) 93.
[21] F. Guimaraes, J. Almeida, J. Bretagne, J. Vac. Sci. Technol., A 9 (1) (1991) 133.
[22] J.W. McConkey, C.P. Malone, P.V. Johnson, C. Winstead, V. McKoy, I. Kanik, Phys. Rep. 466 (2008) 1.
[23] H. Liu, W. Zheng, X. Yan, B. Feng, J. Alloys Compd. 462 (2008) 356.
[24] L. Ai, G. Fang, L. Yuan, N. Liu, M. Wang, C. Li, Q. Zhang, J. Li, X. Zhao, Appl. Surf. Sci. 254 (2008) 2401.
[25] D.-J. Yun, S.-W. Rhee, J. Vac. Sci. Technol., B 26 (5) (2008) 1787.
[26] J.-W. Park, J.-W. Park, D.-Y. Kim, J.-K. Lee, J. Vac. Sci. Technol., A 23 (5) (2005) 1309.
[27] D.A. Wruck, M.A. Dixon, M. Rubin, S.N. Bogy, J. Vac. Sci. Technol., A 9 (4) (1991) 2170.
[28] A. Karpinski, N. Ouldhamadouche, A. Ferrec, L. Cattin, M. Richard-Plouet, L. Brohan, M.A. Djouadi, P.-Y. Jouan, Thin Solid Films 519 (2011) 5767.